Analysis of mRNA multimerisation (aggregation) using non-denaturing ion-pair reversed-phase liquid chromatography

Alexandra L.J. Webb[1], Emma N. Welbourne[1], Thomas C. Minshull[1], Kate A. Loveday[1], Prerna Bora[1], Zoltán Kis[1], Gunilla A. Nilsson[2], Andal Murthy[3], Eivor Örnskov[2] and Mark J. Dickman[1]

[1] *School of Chemical, Materials and Biological Engineering, University of Sheffield, Sheffield, S1 3JD, UK*

[2] *Advanced Drug Delivery, Pharmaceutical Sciences, BioPharmaceuticals R&D, AstraZeneca, Gothenburg, Sweden*

[3] *Purification and Analytical Sciences, Biopharmaceutical Development, AstraZeneca, Cambridge Biomedical Campus, Cambridge CB2 0AA, UK*

Corresponding author: m.dickman@sheffield.ac.uk

Key words: mRNA medicines, Ion-Pair Reversed-Phase HPLC, Mass photometry, mRNA multimers, mRNA aggregates.

Abstract

mRNA-based technology has emerged as a new class of medicines with a wide range of applications, including viral vaccines, cancer vaccines, and therapeutics for the treatment of metabolic diseases and cardiovascular conditions. Impurities, including double-stranded RNA (dsRNA), mRNA fragments, and mRNA multimers (aggregates) that result from the manufacturing of mRNA, as well as from subsequent purification, formulation, and storage, can potentially impact the safety and efficacy of mRNA medicines.

mRNA higher-order structures and mRNA multimers (aggregates) can affect translational efficiency and also impact the efficiency of formulation into lipid nanoparticles. mRNA purity is typically analysed using denaturing or partially denaturing methods, precluding the detection of mRNA multimers (aggregates). In this study, we developed and utilised ion-pair reversed-phase HPLC (IP-RP HPLC) under non-denaturing conditions to analyse mRNA multimers. The inclusion of 1 mM Mg^{2+} in the mobile phase stabilises mRNA higher-order structures, RNA:RNA interactions, and the formation of mRNA dimers/multimers, which can be readily separated from the mRNA monomers.

The ability to resolve mRNA monomers from mRNA dimers/multimers was demonstrated for a range of mRNA sequences and lengths. Moreover, we have shown that the relative abundance of mRNA dimers/multimers is concentration dependent. Using the relative percentage of dimer vs concentration of monomer, we were able to determine that the K_d of the interaction between two eGFP mRNA monomers was 82.93 nM. Characterisation and sizing of the mRNA multimers was performed using mass photometry analysis following the purification of mRNA monomer and dimer/multimer peaks using IP-RP HPLC.

Thus, non-denaturing IP-RP demonstrates significant advantages over current approaches for the analysis of mRNA multimers (aggregates). The high-throughput, temperature-dependent profiling of mRNA multimerisation using IP-RP HPLC will enable further comparative studies on the stability of mRNA multimers and provide important insights into potential factors influencing mRNA multimerisation.

1. Introduction

The global success of the Covid-19 mRNA vaccines has fuelled further research into mRNA vaccines and therapeutics. Beyond vaccines, mRNA medicines have the potential as therapeutics for the treatment of metabolic diseases, cardiovascular disease and cancer vaccines [1–4]. mRNA medicines are routinely manufactured using in vitro transcription (IVT) from a DNA template [5,6]. However, impurities including double-stranded RNA (dsRNA), mRNA fragments, and mRNA multimers (aggregates) that result from the manufacturing of mRNA, as well as from subsequent purification, formulation, and storage, can potentially impact the safety and efficacy of mRNA medicines [2,7–9]. Therefore, robust analytical methods are required for the monitoring of mRNA purity and stability [10,11].

RNA multimerisation, driven by intermolecular RNA:RNA interactions, plays an essential role in organising cellular space. These interactions drive biomolecular condensation, phase separation, and the formation of ribonucleoprotein (RNP) granules [12–14]. The resulting higher-order RNA structures are critical for regulating gene expression, cellular stress responses and viral replication. Together, these findings highlight the biological importance of RNA multimerisation. RNA:RNA interactions that promote multimer formation—most commonly observed in homodimers—include kissing-loop (KL) interactions, complementary base-pairing, and additional tertiary contacts (e.g., minor-groove interactions, A-stacking, and pseudoknot formation) [15,16].

Divalent cations, particularly Mg^{2+}, are critical for stabilising tertiary and quaternary interactions between discrete RNA elements [17,18]. Mg^{2+} counterions both shield electrostatic repulsion from closely orientated phosphate backbones and form site-specific chelated interactions that bridge tertiary contacts. The resulting monomer–dimer populations may exist in either a dynamic equilibrium or a stable, non-interconverting state. The balance and the rate of interconversion are critically influenced by RNA concentration and other environmental conditions, such as temperature, pH, ionic strength, and divalent cation availability [19–21].

mRNA higher-order structures and multimers formed via aggregation can affect translational efficiency [1,2,22] and also impact the efficiency of formulation into lipid nanoparticles [23] and are, therefore, a critical quality attribute (CQA) of the mRNA drug substance. The assessment of mRNA purity includes identifying and quantifying the abundance of mRNA multimers/aggregates from mRNA monomers [10,11,24]. Therefore, analytical methods are

required for the analysis of mRNA multimers/aggregates. Currently, there are limited analytical techniques that both preserve mRNA higher-order structures, noncovalent mRNA interactions during analysis and provide the appropriate resolution of these high molecular weight mRNA species [22].

Size exclusion chromatography (SEC-HPLC) has been utilised for analysis of the structural characteristics, purity, and aggregation states of mRNA, characterising the mRNA in its native form [10,22,25–27]. SEC-UV methods have previously been used to detect the presence of mRNA aggregates in samples of GFP mRNA (980-996 nts) from alternative manufacturers and used to monitor the removal of non-covalently bound species [22]. Multi-angle light scattering (MALS) has been coupled to SEC in order to detect the molecular weight of separated mRNA species [25,28].

SEC-HPLC has previously been used to analyse ssRNA of varying lengths [25]. Due to the large size of typical mRNA medicines, SEC columns with ultrawide pore sizes have been developed to provide adequate resolution for the separation of these large nucleic acids [10,22]. However, SEC-HPLC is typically a low-resolution chromatographic technique and baseline separation of complex mRNA samples is difficult to achieve, even with optimised buffer pH, column oven temperature and pore size (especially for species> 1000 nucleotides) [22,26]. Chromatographic run times can also be long, reducing sample throughput [26]. In addition, microcapillary electrophoresis (mCE) under native conditions has also been employed for the analysis of aggregates in mRNA samples [27]. Improved separation of eGFP mRNA monomers from aggregates using mCE was achieved when compared to SEC-HPLC. Moreover, mCE approaches require significantly reduced analysis times compared to SEC-HPLC and require less sample for analysis. However, further optimisation of mCE methods is needed to improve reproducibility and accuracy, especially given the charged nature and large size, which can cause adsorption to the capillary walls, leading to variation in signal intensity [27].

Mass photometry (MP) has emerged as an additional analytical method capable of measuring mass and relative abundance of nucleic acids in solution. The technique is label-free and measures the mass of single molecules in solution by detecting changes in light scattering as species bind to a glass surface [25,27,29–31]. MP has shown its capability to deliver critical information on various CQAs, including mRNA length [31] and insights into mRNA purity, including the detection of noncovalent species, such as mRNA multimers [26,28]. MP analysis is therefore able to perform purity analysis of native mRNA species, detecting monomers,

multimers and mRNA fragments in 60 seconds. Furthermore, lower amounts of mRNA (~50-100 ng) are required for analysis compared to alternative methods such as SEC and SEC-MALS [27].

In this study, we have developed and utilised non-denaturing IP-RP HPLC in conjunction with the inclusion of 1 mM Mg^{2+} in the mobile phase to study mRNA multimers. The ability to resolve mRNA monomers from mRNA dimers/multimers was demonstrated for a range of different mRNA sequences and lengths. Mass photometry mRNA analysis of the IP RP purified mRNA monomer and dimers/multimers was performed to further characterise and size the mRNA species. Furthermore, quantitative analysis of mRNA multimerisation was carried out across different column temperatures, enabling the relative abundance of mRNA monomers and dimers/multimers to be compared across different mRNAs.

2. Materials and methods

2.1 Chemicals

Triethylammonium acetate (TEAA) (HPLC grade, Glen Research), acetonitrile (ACN) (HPLC grade, Fisher), water (HPLC grade, Fisher), and a 2 M magnesium chloride solution (Sigma) were used to prepare mobile phases for IP-RP HPLC analysis. 1 X PBS solution was prepared for mass photometry from 10 X PBS solution (Fisher) diluted in nuclease-free water. *In vitro* transcription used NTPs (Roche), CleanCap® Reagent AG (BOC), inorganic pyrophosphatase (IPP) (Roche), T7 RNA Polymerase (Roche), HEPES (Gibco), Magnesium acetate (Sigma-Aldrich), DTT (Thermo Fisher), Spermidine (Sigma Aldrich), Triton X-100 (Merck) and lithium chloride solution (7.5 M, Thermo Fisher Scientific). Sodium acetate solution (VWR) and absolute ethanol (Fisher) were used for mRNA precipitation. High-range Riboruler RNA ladder (Thermo Fisher) was used for sizing.

2.2 mRNA sample preparation

In vitro transcription

5 different mRNAs of varying length, including 930 nt (eGFP), 1925 nt (fLuc), 1883 nt, 2098 nt and a 4286 nt mRNA sequence encoding the SARS-CoV-2 spike protein (CSP) were synthesised from linearised plasmid DNA templates (see Table 1). mRNA was prepared using

i*n vitro* transcription (IVT) using linearised DNA template (1 µg), NTPs (10 mM), 5' cap (10 mM), IPP (0.05 U/µL), RNase inhibitor (1 U/µL), T7 polymerase (246.1 U/µL) and nuclease-free water. Reactions were incubated for 2 hrs at 37 ℃.

Lithium chloride purification of mRNA

Lithium chloride (7.5 M) was added to crude mRNA and incubated overnight at -20 ℃. Samples were centrifuged at 13,000 rpm for 20 minutes at 4 °C, supernatant discarded, and the pellet washed twice with ice-cold 80% ethanol. The pellet was resuspended in nuclease-free water.

mRNA precipitation from ion-pair reagent

mRNA was collected post UV detector, and sodium acetate was added to the sample to a final concentration of 0.3 M. 1 volume of ice-cold ethanol was added to the sample and was stored at -80 °C for at least 1 hour. Samples were centrifuged at 13,000 rpm for 20 minutes at 4 °C, supernatant discarded, and the pellet washed twice with ice-cold 80% ethanol. The pellet was resuspended in nuclease-free water.

Heat treatment of mRNA samples prior to IP RP HPLC analysis

Where stated, mRNA samples were heated to 75 °C for 5 minutes and cooled on ice for a further 5 minutes.

2.3 Capillary gel electrophoresis

Capillary gel electrophoresis was performed to determine the size and integrity of mRNA. Analysis was performed on a 5200 Fragment Analyzer system (Agilent). The DNF-471 RNA Kit (15 nt) (Agilent) was used for analysis. This included RNA separation gel, dsDNA inlet buffer, TE rinse buffer, intercalating dye, RNA diluent marker (15 nt), RNA ladder (from 200 to 6000 nt) and capillary conditioning solution. A FA 12-Capillary Array Short, 33 cm capillary cassette was used (Agilent). Fluorescence detection was used in conjunction with an intercalating dye in the separation gel. RNA samples were heated to 70 °C for 5 minutes and cooled on ice prior to analysis [31]. The integrity was determined based on the peak area of the full-length intact mRNA and total peak areas, including the smaller degraded RNA (see Table 1).

2.4 IP-RP HPLC analysis

IP-RP HPLC analysis of mRNA was performed using U3000 and Vanquish HPLC systems (Thermo Fisher) using a DNAPac RP 2.1 x 100 mm or a ProSwift 1S 4.6 X 50 mm (Thermo Fisher). Mobile phase A was 0.1 M TEAA, and mobile phase B was 0.1 M TEAA, 25% ACN. Alternative mobile phases for the native IP-RP HPLC were prepared by the addition of magnesium chloride to a final concentration of 1 mM Mg^{2+} in mobile phases A and B.

HPLC separations were performed using the following gradients:

Gradient 1: Mobile phase A was 0.1 M TEAA, and mobile phase B was 0.1 M TEAA, 25% ACN. The gradient consisted of a linear step from 25-30% over 1 minute, followed by a convex extension (curve 3) to 65% B over 14 minutes, flow rate 0.25 mL/min, UV detection at 260 nm.

Gradient 2: Mobile phase A was 0.1 M TEAA + 1 mM $Mg^{2+,}$ and mobile phase B was 0.1 M TEAA, 1 mM $Mg^{2+,}$ 25% ACN. The gradient consisted of a linear step from 15-20% over 1 minute, followed by a convex extension (curve 3) to 70% B over 14 minutes, flow rate 0.2 (DNAPac RP 2.1 x 100 mm) or 0.50 mL/min (ProSwift 1S 4.6 X 40 mm), UV detection at 260 nm.

For convex gradients:

$$Ve = Vf - 2(Vt - Vf)\left(\frac{2^{\frac{-10(Te-Tf)}{(Tt-Tf)}}}{1-2^{-10}}\right) + \frac{3(Vt-Vf)(Te-Tf)}{(Tt-Tf)}$$

2.5 K_d determination

An 8 point concentration curve was used to determine K_d: 16.15 nM, 32.3 nM, 64.6 nM, 129.2 nM, 193.8 nM, 258.38 nM, 322.98 nM, 645.96 nM. The relative abundance of the dimer (% area) was plotted against concentration, and the K_d was determined by non-linear regression analysis using the Specific Binding with Hill Slope equation in GraphPad Prism version 10.5.0.

2.6 Mass photometry analysis

Analysis of mRNA was performed using a TwoMP mass photometer (Refeyn). Glass coverslips, 24 x 50 mm, (Epredia, UK) were rinsed with Milli-Q water, methanol and then isopropanol (repeated twice) and dried under nitrogen. Glass coverslips were then submerged in 0.01% poly-L-lysine (PLL) for 5 mins for coating and left overnight to dry under nitrogen. RNA samples were diluted in 1X PBS solution to approximately 10 ng/μL and left at room temperature for 10 minutes before analysis. Droplet-free dilution using 1 X PBS solution was performed prior to sample measurement. Data was acquired for 60 seconds after the addition of RNA. Riboruler High Range RNA Ladder (ThermoFisher) was used as the calibration standard to perform mRNA sizing. Acquire MP and Discover MP software (Refeyn) were used to acquire and analyse data.

3. Results and Discussion

3.1 Separation of mRNA monomers and dimers (multimers) using non-denaturing IP-RP HPLC

mRNAs with a wide range of sizes were synthesised using *in vitro* transcription for this study, including a 930 nt (eGFP), 1925 nt (fLuc), 1883 nt, 2098 nt and a 4286 nt mRNA encoding the SARS-CoV-2 spike protein (CSP). A summary of all mRNA used in this study is shown in Table 1. The integrity of the mRNA was determined by capillary gel electrophoresis and IP-RP HPLC under denaturing conditions (70 °C) (see Supplementary Figure S1/S2). All mRNAs used in this study had an integrity of >90% (see Table 1), with good agreement between the IP-RP HPLC and CE analysis. However, analysis under denaturing (partially denaturing) methods such as capillary electrophoresis and denaturing IP-RP-HPLC prevents the analysis of mRNA higher-order structures, including non-covalent mRNA multimers or potential dsRNA impurities. As expected, under the typical denaturing conditions of CE and IP-RP, only minor peaks to the right-hand side of the full-length mRNA were observed ((see Supplementary Figure S1/S2).

Previous work has shown that RNA molecules form multimers that are stable under non-denaturing analytical methods such as non-denaturing agarose gel electrophoresis [32,33], SEC [25,27,28] and mass photometry [25,30,31]. Therefore, further work was performed to develop alternative native chromatographic conditions that enable the analysis of mRNA higher-order

structures, including the presence of mRNA multimers. Initial work showed that using low temperature in conjunction with IP-RP HPLC using TEAA mobile phases resulted in the presence of only a single peak corresponding to the full-length mRNA. The folding of RNA molecules, stabilisation of RNA secondary structures, and RNA:RNA interactions is dependent on the presence of divalent metal ions [34]. We have previously utilised and developed IP-RP HPLC in the presence of Mg^{2+} ions for the analysis of the human telomerase RNA (hTR) [35]. These results demonstrated that, in the presence of Mg^{2+} ions, the dimer (or multimeric) hTR RNA species is stabilised and elutes later than the monomer [35]. Free Mg^{2+} concentration inside cells is approximately 0.5-1.2 mM [36,37]. Therefore, reflecting the physiological free Mg^{2+} concentration, ion-pair mobile phases were used with the addition of 1 mM Mg^{2+} for the analysis of mRNA and their higher-order structures/multimers. Initial work focussed on using TEAA mobile phase with the addition of 1 mM Mg^{2+} in conjunction with stationary phases with macro-porous particles and monolithic PS-DVB columns, which enables the high-resolution separation of large RNA (>1000 nt) [38,39]. The addition of 1 mM Mg^{2+} to TEAA mobile phases did not alter the resolution or cause column stability issues as demonstrated by the separation of a 100 bp DNA ladder (see Supplementary Figure S3).

Analysis of eGFP mRNA using non-denaturing IP-RP HPLC across varying column temperatures is shown in Figure 1A. The results show that the presence of two major peaks is seen at lower column temperatures (40 and 50 ℃) and only a single peak is observed at higher temperatures (> 60 ℃). It is proposed that in the presence of Mg^{2+} and temperatures <60 ℃, RNA:RNA interactions are stabilised. This results in a later elution time than the corresponding mRNA monomer, as observed at 40/50 ℃ for eGFP mRNA. In addition to the abundant proposed mRNA monomer and dimer peaks, later eluting peaks are also observed at 40/50 ℃ corresponding to proposed mRNA multimers. The disruption of these weak RNA:RNA interactions by increasing temperatures yields a single chromatographic peak, consistent with the presence of only the mRNA monomer (see Figure 1A).

To further characterise the proposed mRNA dimer/multimers, the two peaks observed during initial IP-RP HPLC separation were collected. These fractions were subsequently re-injected onto the IP-RP HPLC column directly (see Figure 1B/C). Re-injection of Peak 1 (mRNA monomer) and Peak 2 (mRNA dimer) at 45 ℃ resulted in retention times consistent with their original elution. Thus demonstrating the multimeric mRNA is stable following IP-RP HPLC purification. Furthermore, at 60 ℃, a complete shift in the retention time of peak 2 is observed,

aligning with the retention time of peak 1 (see Figure 1C). This is consistent with the complete dissociation of a non-covalently assembled mRNA multimer at the elevated temperatures.

In addition, alternative mobile phases were also employed, including stronger IP reagents, including hexylammonium acetate (HAA) (10 mM HAA + 1 mM Mg^{2+}). However, under these conditions, lower resolution separation of larger RNAs and mRNA dimers/multimers was observed (see Supplementary Figure S4). Furthermore, using stronger IP reagents such as HAA requires a higher concentration of organic modifier to elute the RNA, which may also result in denaturation of the mRNA multimers.

3.2 Mass Photometry analysis of mRNA multimers purified using IP-RP HPLC

Mass photometry (MP) was used to characterise and size the corresponding mRNA species (monomer and dimer/multimer) isolated directly from IP-RP HPLC. Sizing of the eGFP mRNA was performed following calibration using a ssRNA ladder (200-6000 nts), demonstrating the ability of MP to accurately determine the size of the mRNA. The MP data for eGFP mRNA (prior to IP-RP HPLC purification) reveals additional, less abundant mRNA species of increased size, consistent with mRNA dimers or multimers (Supplementary Figure S5). Following IP-RP HPLC at 55 °C, the corresponding peaks (1 and 2) were collected and analysed directly using MP (see Figure 2). The results showed that peak 1 corresponds to the eGFP monomer, and peak 2 showed the presence of multiple RNA species, with the most abundant corresponding to the mRNA dimer. It is interesting to note that the data also showed the presence of the mRNA trimer that was not observed from the mRNA monomer purified using IP-RP HPLC (see Figure 2).

Following confirmation using MP that the additional peaks observed in the non-denaturing IP-RP HPLC correspond to the eGFP mRNA dimers/multimers, further work was performed to optimise the separation and fractionation of the eGFP mRNA monomer, dimer and multimers. Fractionation of the central apex of the mRNA monomer and dimer peaks and an expanded fraction of the mRNA multimers was performed (see Figure 2C). MP was subsequently used to characterise and size these fractions (see Figure 2D). The results show that only the mRNA monomer was observed in peak 1, and predominantly the mRNA dimer was observed in peak 2. Furthermore, the results show that for the peak (3), a wide range of mRNA multimers were identified, including trimer, tetramers, pentamers and hexamers for eGFP mRNA.

3.3 mRNA concentration affects multimerisation

The formation of protein multimers (dimers, trimers, etc.) is concentration-dependent, with higher concentrations generally favouring multimer formation [40–42]. Therefore, to further study the effects of mRNA concentration on multimerisation, a range of different concentrations (5 ng/µL (16.1 nM) to 200 ng/µL (645.9 6nM)) of eGFP mRNA were analysed using IP-RP HPLC in the presence of magnesium (Figure 3). A significant difference in the relative amounts of mRNA dimer (multimer) analysed at 54 °C comparing a low concentration of mRNA (5 ng/µL) where little or no mRNA dimer (multimer) (91.0% monomer, 9.0% multimers) is observed compared to the higher concentration (200 ng/µL) where the majority of the mRNA is present as dimers (multimers) with little or no monomer observed (14.3% monomer, 85.7% multimers) (see Figure 3B).

Using the relative percentage of dimer vs concentration of monomer, we were able to determine that the K_d of the interaction between two eGFP mRNA monomers was 82.93 nM (Figure 3C). As the concentration of purified dimer from the IP-RP HPLC (~16.1 nM) used for MP is lower than the K_d, this likely explains the presence of monomer in the purified dimer peak (peak 2) (see Figure 2D).

These results demonstrate that increasing eGFP mRNA concentration promotes the formation of mRNA dimers and multimers, a finding consistent with the concentration-dependent multimerisation observed for a range of RNAs [43,44]. Moreover, the ability to inject a wide range of different concentrations of mRNA highlights the ability to study the effect of concentration using IP-RP HPLC, which is not possible using mass photometry, where typically low concentrations of RNA are required for analysis.

Further studies were performed by injecting different volumes of mRNA from the same concentration to study the effect of analysing different masses of mRNA (see Supplementary Figure S6). No difference in mRNA multimerisation was observed, demonstrating that mRNA multimerisation is independent of mass analysed on the IP-RP HPLC and varies with mRNA concentration.

3.4 Heat denaturation of mRNA samples prior to mRNA analysis of mRNA multimers.

To further investigate the mRNA multimers and their potential dynamic equilibrium, the mRNA sample was heat-denatured (75 °C for 5 minutes) immediately before analysis by non-denaturing IP-RP HPLC. Following the previous results that showed the relationship between mRNA concentration and mRNA multimerisation, experiments were performed using heat denaturation of the mRNA samples across a range of different mRNA concentrations (see Figure 4A). At a low eGFP mRNA concentration (10 ng/µL), heat denaturation of the mRNA reduced the relative amount of dimers and multimers, an effect observed across all column temperatures tested. These results are consistent with previous data obtained using heat denaturation prior to SEC analysis of mRNA [22,25]. However, at higher mRNA concentrations, mRNA dimers (multimers) were still present, indicating that this step did not result in the complete removal of the mRNA multimers. The non-denaturing IP-RP HPLC analysis across different column temperatures studied was consistent with previous observations for eGFP mRNA.

Interestingly, IP-RP HPLC analysis at 54 ℃ showed the highest relative abundance of mRNA dimer, indicating the temperature dependence on mRNA dimerisation (see Figure 4B). Indeed, mRNA is known to have complex thermal unfolding pathways, with many closely spaced transitions likely indicating closely related unfolding intermediates [45]. It is plausible that, analogous to protein behaviour, these partially unfolded states may be populated to a higher degree at elevated temperatures, allowing more dimerisation or oligomerisation to occur [46–48]. It is important to note that the mRNA sample experiences a distinct thermodynamic environment, reflecting both the column temperature in combination with the pressure during the HPLC. This is likely to reduce the effective thermal energy experienced by the molecule compared to a sample heated at atmospheric pressure.

In addition, further experiments were performed by heat-denaturing the mRNA sample prior to IP-RP HPLC analysis of the mRNA sample over a prolonged time period to study if the population of the mRNA monomer and multimers changes over time (see Supplementary Figure S7). No significant change in the population of the mRNA dimers/multimers is observed over time, therefore demonstrating that there is a rapid equilibrium of the mRNA monomer/dimer in solution or under the chromatography conditions consistent with previous observations.

3.5 Applications of non-denaturing IP-RP HPLC for the analysis of mRNA multimerisation

Following optimisation of the separation and the temperature-dependent analysis of eGFP mRNA multimers using non-denaturing IP-RP HPLC, further studies were employed to analyse a variety of alternative mRNAs, including a 1925 nt mRNA (fLuc), 1883 nt, 2098 nt mRNA and 4286 nt mRNA (CSP) (see Figure 5). Separation of the mRNA monomer from mRNA dimer/multimers was seen in a temperature-dependent manner, consistent with eGFP mRNA. Clear differences are observed for the IP-RP chromatograms for each of the different mRNAs, reflecting the relative abundance of mRNA monomer and mRNA dimer (multimers) present in each sample at the concentrations analysed. In particular, the 1925 nt mRNA (fLuc) shows a higher relative abundance of mRNA multimers in comparison to the 2098 nt mRNA. Mass photometry (MP) analysis, following the isolation and purification of the corresponding IP-RP HPLC peaks, confirmed that mRNA dimer/multimers are present in each of the later-eluting fractions across all different mRNAs analysed (see Figure 6).

For the IP-RP HPLC-purified multimer peak of the 1883 nt mRNA, MP analysis shows the presence of multiple higher-order species, including dimer, trimer, and tetramer. In contrast, only the monomer was identified in the purified mRNA (peak 1). MP analysis also supports the IP-RP chromatographic data, showing that the purified 1925-nt fLuc mRNA contains a higher relative abundance of multimeric species, notably trimers and tetramers. These results demonstrate the application of the non-denaturing IP-RP HPLC to rapidly determine and compare the relative abundance of mRNA multimers to monomers present in mRNA samples and provide important further insight into the stability of the non-covalent mRNA multimers by comparing their relative abundance at specific temperatures in the non-denaturing IP-RP HPLC. Further optimisation of the mobile phases, gradients and stationary phases will enable improved separation of the mRNA monomers from dimers/multimers for larger mRNAs, which is currently challenging.

4. Conclusions

We have developed and utilised IP-RP HPLC under non-denaturing conditions to analyse mRNA multimers (aggregates). The inclusion of 1 mM Mg^{2+} in the mobile phase stabilises mRNA higher-order structures and RNA:RNA interactions, allowing their separation from monomers and relative quantification by IP-RP HPLC. The ability to resolve mRNA monomers from mRNA dimers/multimers was demonstrated for a range of mRNA sequences and lengths. Moreover, mRNA multimerisation was shown to be concentration dependent. These results demonstrate the importance of analysing mRNA multimerisation (aggregation) over a wide range of mRNA concentrations. In addition, when comparing mRNA multimers (aggregates) from different manufacturing batches or different suppliers, it is important that accurate quantification of the mRNA is performed using the same method or orthogonal methods prior to analysis. Typical mRNA concentrations can reach >1 μg/μL during in vitro transcription reactions. At these concentrations, the relative abundance of mRNA dimers/multimers is expected to be higher than that of mRNA monomers. Furthermore, the relative abundance of mRNA dimers was shown unexpectedly to increase with temperature until a threshold was reached, beyond which denaturation of the mRNA dimer to mRNA monomer then occurred. These results suggest that at a certain temperature, the mRNA adopts a specific higher-order structure(s) that facilitates the dimer formation.

The ability to readily purify the mRNA monomers and dimers/multimers enables further characterisation and downstream studies. Further characterisation and sizing of mRNA multimers was directly performed using mass photometry analysis following the purification of mRNA monomer and dimer/multimer peaks using IP-RP HPLC. The ability to resolve mRNA monomers from mRNA dimers/multimers in short chromatographic run times for further downstream analysis demonstrates significant advantages over current approaches for the analysis of mRNA multimers (aggregates). In addition, we demonstrate the importance of performing the analysis over a wide range of temperatures and concentrations of mRNA to analyse mRNA multimerisation (aggregation). The high-throughput, temperature-dependent profiling of mRNA multimerisation using IP-RP HPLC will enable further comparative studies on the stability of mRNA multimers and provide important insights into potential factors influencing mRNA multimerisation.

Acknowledgements

A.L.J.W is funded by an Engineering and Physical Sciences Research Council (EPSRC) Doctoral Training Partnership CASE Conversion award (EP/W524360/1) in collaboration with AstraZeneca. M.J.D and Z.K acknowledge funding from the Wellcome Leap R3 programme and Coalition for Epidemic Preparedness Innovations (CEPI). MJD acknowledges additional funding from the Biotechnology and Biological Sciences Research Council (BB/Z515930/1).

Conflict of interest

G.A.N., A.M. and E.Ö. are employees of AstraZeneca. All other authors declare no competing interests.

Legends to Figures:

Figure 1 Non-denaturing IP-RP HPLC separation of mRNA multimers. A) IP-RP chromatograms for the analysis of mRNA (eGFP 930 nt) showing the temperature dependent separation of the mRNA monomer from the mRNA dimer (multimers). B/C) IP-RP chromatograms of purified eGFP mRNA peak 1 (monomer) and peak 2 (dimer/multimer) purified at 50 °C, re-injected at varying temperatures (45-60 °C). HPLC separations were performed using gradient 2, UV detection at 260 nm.

Figure 2 Mass Photometry analysis of mRNA multimers. A) IP-RP chromatograms for the analysis of eGFP mRNA (40 ng/µL) following heat denaturation (75 °C, 5 mins) at 55 °C. B) Mass Photometry analysis of peak 1 (>98% monomer) and peak 2 (dimer) purified using IP-RP HPLC. The corresponding % monomer, dimer and trimer were determined based on the calculated size of the mRNA and counts from the mass photometer. C) IP-RP chromatograms for the analysis of eGFP mRNA (200 ng/µL) at 40 °C. D) Mass Photometry analysis of peak 1 (100% monomer), peak 2 (>90% dimer) and peak 3 (multimers) purified using IP-RP HPLC. The corresponding % monomer, dimer and multimers were determined based on the calculated size of the mRNA and counts from the mass photometer.

Figure 3 Concentration effects on mRNA multimerisation. A) IP-RP chromatograms for the analysis of selected concentrations of eGFP mRNA (5, 40 and 200 ng/µL). B) Overlaid IP-RP chromatograms of a wide range of eGFP mRNA concentrations (5-200 ng/µL). IP-RP separations were performed using gradient 2 with UV detection at 260 nm. The corresponding mRNA monomer and mRNA dimer (multimers) are highlighted, including their relative abundance. C) % mRNA dimer concentration curve. Corresponding peak areas for the mRNA monomer and dimer were used to determine the % mRNA dimer for each mRNA concentration. The K_d was determined by non-linear regression analysis using the Specific Binding with Hill Slope equation.

Figure 4 IP-RP HPLC mRNA multimerisation of heat-denatured eGFP mRNA. IP-RP chromatograms for the analysis of eGFP mRNA (10, 40 and 200 ng/µL) following heat denaturation (75 °C, 5 mins) prior to direct analysis over a range of different column temperatures (45, 50 and 60 °C). The corresponding eGFP mRNA with no heat treatment is

shown in purple. B) IP-RP chromatograms for the analysis of eGFP mRNA (40 ng/μL) following heat denaturation (75 °C, 5 mins) prior to direct analysis over a range of different column temperatures (45-60 °C). IP RP separations were performed using gradient 1 with UV detection at 260 nm.

Figure 5. IP-RP HPLC analysis of mRNA multimerisation. IP-RP chromatograms for the analysis of different mRNA sequences showing the temperature dependent separation of the mRNA monomer from the mRNA dimer (multimers). A) 1883 nt mRNA. B) 2098 nt mRNA. C) 1925 nt mRNA. D) 4286 nt mRNA. IP-RP separations were performed using gradient 1 with UV detection at 260nm. The corresponding mRNA monomer and mRNA dimer (multimers) are highlighted.

Figure 6. Mass Photometry analysis of mRNA multimers. A) IP-RP chromatograms for the analysis of 1883 nt mRNA at 50 °C. B) Mass Photometry analysis of peak 1 (monomer) and peak 2 (dimer) purified using IP-RP HPLC. The corresponding % monomer and dimer/trimer were determined based on the calculated size of the mRNA and counts from the mass photometer. A) IP-RP chromatograms for the analysis of 2098 nt mRNA at 40 °C. B) Mass photometry analysis of peak 1 (monomer) and peak 2 (dimer) purified using IP-RP HPLC. The corresponding % monomer and dimer/trimer were determined based on the calculated size of the mRNA and counts from the mass photometer.

References

[1] S. Qin, X. Tang, Y. Chen, K. Chen, N. Fan, W. Xiao, Q. Zheng, G. Li, Y. Teng, M. Wu, X. Song, mRNA-based therapeutics: powerful and versatile tools to combat diseases, Signal Transduct. Target. Ther. 7 (2022) 166. https://doi.org/10.1038/s41392-022-01007-w.

[2] Y.-S. Wang, M. Kumari, G.-H. Chen, M.-H. Hong, J.P.-Y. Yuan, J.-L. Tsai, H.-C. Wu, mRNA-based vaccines and therapeutics: an in-depth survey of current and upcoming clinical applications, J. Biomed. Sci. 30 (2023) 84. https://doi.org/10.1186/s12929-023-00977-5.

[3] H. Zogg, R. Singh, S. Ro, Current Advances in RNA Therapeutics for Human Diseases, Int. J. Mol. Sci. 23 (2022) 2736. https://doi.org/10.3390/ijms23052736.

[4] J.D. Beck, D. Reidenbach, N. Salomon, U. Sahin, Ö. Türeci, M. Vormehr, L.M. Kranz, mRNA therapeutics in cancer immunotherapy, Mol. Cancer 20 (2021) 69. https://doi.org/10.1186/s12943-021-01348-0.

[5] B. Beckert, B. Masquida, Synthesis of RNA by In Vitro Transcription, in: H. Nielsen (Ed.), RNA, Humana Press, Totowa, NJ, 2011: pp. 29–41. https://doi.org/10.1007/978-1-59745-248-9_3.

[6] J. Boman, T. Marušič, T.V. Seravalli, J. Skok, F. Pettersson, K.Š. Nemec, H. Widmark, R. Sekirnik, Quality by design approach to improve quality and decrease cost of in vitro transcription of mRNA using design of experiments, Biotechnol. Bioeng. (2024) bit.28806. https://doi.org/10.1002/bit.28806.

[7] K. Karikó, H. Muramatsu, F.A. Welsh, J. Ludwig, H. Kato, S. Akira, D. Weissman, Incorporation of Pseudouridine Into mRNA Yields Superior Nonimmunogenic Vector With Increased Translational Capacity and Biological Stability, Mol. Ther. 16 (2008) 1833–1840. https://doi.org/10.1038/mt.2008.200.

[8] U. Sahin, K. Karikó, Ö. Türeci, mRNA-based therapeutics — developing a new class of drugs, Nat. Rev. Drug Discov. 13 (2014) 759–780. https://doi.org/10.1038/nrd4278.

[9] X. Hou, T. Zaks, R. Langer, Y. Dong, Lipid nanoparticles for mRNA delivery, Nat. Rev. Mater. 6 (2021) 1078–1094. https://doi.org/10.1038/s41578-021-00358-0.

[10] USP, Analytical Procedures for Quality of mRNA Vaccines and Therapeutics, 3rd Edition (2024).

[11] European Medicines Agency, Guideline on the quality aspects of mRNA vaccines (Draft), Chrome-Extensionefaidnbmnnnibpcajpcglclefindmkajhttpswwwemaeuropaeuendocumentsscient Ific-Guidel.-Guidel.-Qual.-Asp.-Mrna-Vaccinesenpdf (2025).

[12] A. Khong, T. Matheny, S. Jain, S.F. Mitchell, J.R. Wheeler, R. Parker, The Stress Granule Transcriptome Reveals Principles of mRNA Accumulation in Stress Granules, Mol. Cell 68 (2017) 808-820.e5. https://doi.org/10.1016/j.molcel.2017.10.015.

[13] B. Van Treeck, R. Parker, Emerging Roles for Intermolecular RNA-RNA Interactions in RNP Assemblies, Cell 174 (2018) 791–802. https://doi.org/10.1016/j.cell.2018.07.023.

[14] S. Guil, M. Esteller, RNA–RNA interactions in gene regulation: the coding and noncoding players, Trends Biochem. Sci. 40 (2015) 248–256. https://doi.org/10.1016/j.tibs.2015.03.001.

[15] C. Bou-Nader, J. Zhang, Structural Insights into RNA Dimerization: Motifs, Interfaces and Functions, Molecules 25 (2020) 2881. https://doi.org/10.3390/molecules25122881.

[16] I. Skeparnias, J. Zhang, Cooperativity and Interdependency between RNA Structure and RNA–RNA Interactions, Non-Coding RNA 7 (2021) 81. https://doi.org/10.3390/ncrna7040081.

[17] E. Ding, S.N. Chaudhury, J.D. Prajapati, J.N. Onuchic, K.Y. Sanbonmatsu, Magnesium ions mitigate metastable states in the regulatory landscape of mRNA elements, RNA 30 (2024) 992–1010. https://doi.org/10.1261/rna.079767.123.

[18] D. Grilley, A.M. Soto, D.E. Draper, Mg^{2+} –RNA interaction free energies and their relationship to the folding of RNA tertiary structures, Proc. Natl. Acad. Sci. 103 (2006) 14003–14008. https://doi.org/10.1073/pnas.0606409103.

[19] R. Guth-Metzler, A.M. Mohamed, E.T. Cowan, A. Henning, C. Ito, M. Frenkel-Pinter, R.M. Wartell, J.B. Glass, L.D. Williams, Goldilocks and RNA: where Mg2+ concentration is just right, Nucleic Acids Res. 51 (2023) 3529–3539. https://doi.org/10.1093/nar/gkad124.

[20] J.H. Davis, T.R. Foster, M. Tonelli, S.E. Butcher, Role of metal ions in the tetraloop–receptor complex as analyzed by NMR, RNA 13 (2007) 76–86. https://doi.org/10.1261/rna.268307.

[21] X. Sun, J.M. Li, R.M. Wartell, Conversion of stable RNA hairpin to a metastable dimer in frozen solution, RNA 13 (2007) 2277–2286. https://doi.org/10.1261/rna.433307.

[22] A. Goyon, S. Tang, S. Fekete, D. Nguyen, K. Hofmann, S. Wang, W. Shatz-Binder, K.I. Fernandez, E.S. Hecht, M. Lauber, K. Zhang, Separation of Plasmid DNA Topological Forms, Messenger RNA, and Lipid Nanoparticle Aggregates Using an Ultrawide Pore Size Exclusion Chromatography Column, Anal. Chem. 95 (2023) 15017–15024. https://doi.org/10.1021/acs.analchem.3c02944.

[23] J.D. Beck, D. Reidenbach, N. Salomon, U. Sahin, Ö. Türeci, M. Vormehr, L.M. Kranz, mRNA therapeutics in cancer immunotherapy, Mol. Cancer 20 (2021) 69. https://doi.org/10.1186/s12943-021-01348-0.

[24] M. Kloczewiak, J.M. Banks, L. Jin, M.L. Brader, A Biopharmaceutical Perspective on Higher-Order Structure and Thermal Stability of mRNA Vaccines, Mol. Pharm. 19 (2022) 2022–2031. https://doi.org/10.1021/acs.molpharmaceut.2c00092.

[25] J. De Vos, K. Morreel, P. Alvarez, H. Vanluchene, R. Vankeirsbilck, P. Sandra, K. Sandra, Evaluation of size-exclusion chromatography, multi-angle light scattering detection and mass photometry for the characterization of mRNA, J. Chromatogr. A 1719 (2024) 464756. https://doi.org/10.1016/j.chroma.2024.464756.

[26] V. D'Atri, H. Lardeux, A. Goyon, M. Imiołek, S. Fekete, M. Lauber, K. Zhang, D. Guillarme, Optimizing Messenger RNA Analysis Using Ultra-Wide Pore Size Exclusion Chromatography Columns, Int. J. Mol. Sci. 25 (2024) 6254. https://doi.org/10.3390/ijms25116254.

[27] J. Camperi, S. Lippold, L. Ayalew, B. Roper, S. Shao, E. Freund, A. Nissenbaum, C. Galan, Q. Cao, F. Yang, C. Yu, A. Guilbaud, Comprehensive Impurity Profiling of mRNA: Evaluating Current Technologies and Advanced Analytical Techniques, Anal. Chem. 96 (2024) 3886–3897. https://doi.org/10.1021/acs.analchem.3c05539.

[28] P. Wang, R. Akula, M. Chen, K. Legaspi, AN1616: SEC-MALS Method for Characterizing mRNA Biophysical Attributes, Wyatt Technol. Appl. Note (n.d.).

[29] C. Wagner, F.F. Fuchsberger, B. Innthaler, M. Lemmerer, R. Birner-Gruenberger, Quantification of Empty, Partially Filled and Full Adeno-Associated Virus Vectors Using Mass Photometry, Int. J. Mol. Sci. 24 (2023) 11033. https://doi.org/10.3390/ijms241311033.

[30] E. Deslignière, L.F. Barnes, T.W. Powers, O.V. Friese, A.J.R. Heck, Characterization of intact mRNA-based therapeutics by charge detection mass spectrometry and mass photometry, Mol. Ther. Methods Clin. Dev. 33 (2025) 101454. https://doi.org/10.1016/j.omtm.2025.101454.

[31] A. Schmudlach, S. Spear, Y. Hua, S. Fertier-Prizzon, J. Kochling, Mass photometry as a fast, facile characterization tool for direct measurement of mRNA length, Biol. Methods Protoc. 10 (2025) bpaf021. https://doi.org/10.1093/biomethods/bpaf021.

[32] X. Ren, Identification of a new RNA{middle dot}RNA interaction site for human telomerase RNA (hTR): structural implications for hTR accumulation and a dyskeratosis congenita point mutation, Nucleic Acids Res. 31 (2003) 6509–6515. https://doi.org/10.1093/nar/gkg871.

[33] H. Ly, L. Xu, M.A. Rivera, T.G. Parslow, E.H. Blackburn, A role for a novel ‘ *trans* -pseudoknot’ RNA–RNA interaction in the functional dimerization of human telomerase, Genes Dev. 17 (2003) 1078–1083. https://doi.org/10.1101/gad.1060803.

[34] V.K. Misra, D.E. Draper, On the role of magnesium ions in RNA stability, Biopolymers 48 (1998) 113–135. https://doi.org/10.1002/(SICI)1097-0282(1998)48:2%253C113::AID-BIP3%253E3.0.CO;2-Y.

[35] S.P. Waghmare, P. Pousinis, D.P. Hornby, M.J. Dickman, Studying the mechanism of RNA separations using RNA chromatography and its application in the analysis of ribosomal RNA and RNA:RNA interactions, J. Chromatogr. A 1216 (2009) 1377–1382. https://doi.org/10.1016/j.chroma.2008.12.077.

[36] A.R. Morrison, Magnesium Homeostasis: Lessons from Human Genetics, Clin. J. Am. Soc. Nephrol. 18 (2023) 969–978. https://doi.org/10.2215/CJN.0000000000000103.

[37] H. Ebel, T. Günther, Magnesium Metabolism: A Review, Cclm 18 (1980) 257–270. https://doi.org/10.1515/cclm.1980.18.5.257.

[38] M. Ozaki, T. Kuwayama, M. Shimotsuma, T. Hirose, Separation and purification of short-, medium-, and long-stranded RNAs by RP-HPLC using different mobile phases and C_{18} columns with various pore sizes, Anal. Methods 16 (2024) 1948–1956. https://doi.org/10.1039/D4AY00114A.

[39] J. Currie, J.R. Dahlberg, E. Lundberg, L. Thunberg, J. Eriksson, F. Schweikart, G.A. Nilsson, E. Örnskov, Stability indicating ion-pair reversed-phase liquid chromatography method for modified mRNA, J. Pharm. Biomed. Anal. 245 (2024) 116144. https://doi.org/10.1016/j.jpba.2024.116144.

[40] S. Yadav, J. Liu, S.J. Shire, D.S. Kalonia, Specific interactions in high concentration antibody solutions resulting in high viscosity, J. Pharm. Sci. 99 (2010) 1152–1168. https://doi.org/10.1002/jps.21898.

[41] S.V. Sule, M. Sukumar, W.F. Weiss, A.M. Marcelino-Cruz, T. Sample, P.M. Tessier, High-Throughput Analysis of Concentration-Dependent Antibody Self-Association, Biophys. J. 101 (2011) 1749–1757. https://doi.org/10.1016/j.bpj.2011.08.036.

[42] J. Liu, M.D.H. Nguyen, J.D. Andya, S.J. Shire, Reversible Self-Association Increases the Viscosity of a Concentrated Monoclonal Antibody in Aqueous Solution, J. Pharm. Sci. 94 (2005) 1928–1940. https://doi.org/10.1002/jps.20347.

[43] D. Ishimaru, E.P. Plant, A.C. Sims, B.L. Yount, B.M. Roth, N.V. Eldho, G.C. Pérez-Alvarado, D.W. Armbruster, R.S. Baric, J.D. Dinman, D.R. Taylor, M. Hennig, RNA dimerization plays a role in ribosomal frameshifting of the SARS coronavirus, Nucleic Acids Res. 41 (2013) 2594–2608. https://doi.org/10.1093/nar/gks1361.

[44] T. Chkuaseli, K.A. White, Dimerization of an umbravirus RNA genome activates subgenomic mRNA transcription, Nucleic Acids Res. 51 (2023) 8787–8804. https://doi.org/10.1093/nar/gkad550.

[45] M. Kloczewiak, J.M. Banks, L. Jin, M.L. Brader, A Biopharmaceutical Perspective on Higher-Order Structure and Thermal Stability of mRNA Vaccines, Mol. Pharm. 19 (2022) 2022–2031. https://doi.org/10.1021/acs.molpharmaceut.2c00092.

[46] A. Chadli, M.M. Ladjimi, E.-E. Baulieu, M.G. Catelli, Heat-induced Oligomerization of the Molecular Chaperone Hsp90, J. Biol. Chem. 274 (1999) 4133–4139. https://doi.org/10.1074/jbc.274.7.4133.

[47] J.C. Woodard, S. Dunatunga, E.I. Shakhnovich, A Simple Model of Protein Domain Swapping in Crowded Cellular Environments, Biophys. J. 110 (2016) 2367–2376. https://doi.org/10.1016/j.bpj.2016.04.033.

[48] H. Koss, B. Honig, L. Shapiro, A.G. Palmer, Dimerization of Cadherin-11 involves multi-site coupled unfolding and strand swapping, Structure 29 (2021) 1105-1115.e6. https://doi.org/10.1016/j.str.2021.06.006.

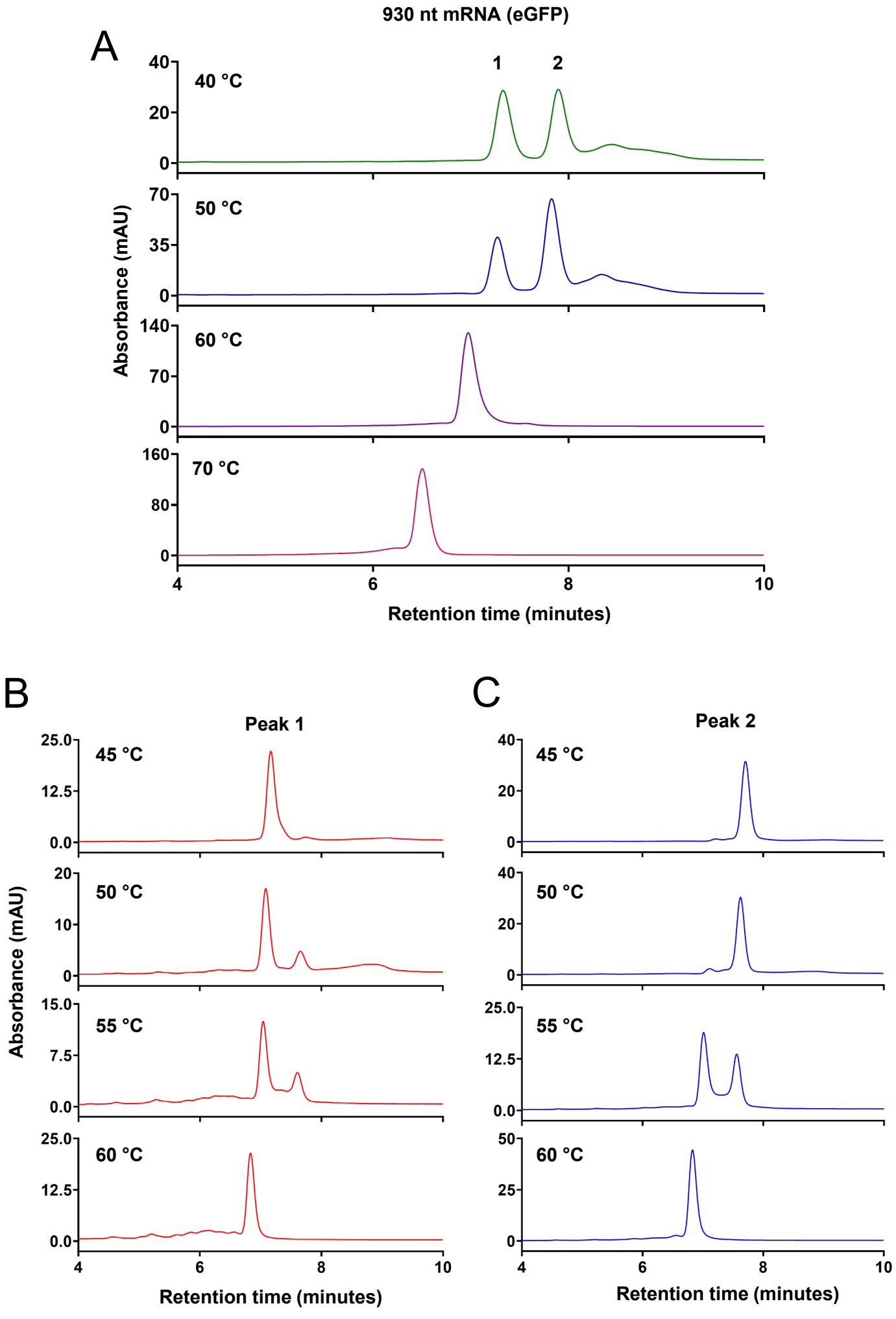
A
930 nt mRNA (eGFP)
1
2
40 °C
50 °C
60 °C
70 °C
Absorbance (mAU)
Retention time (minutes)
B
Peak 1
45 °C
50 °C
55 °C
60 °C
Absorbance (mAU)
Retention time (minutes)
C
Peak 2
45 °C
50 °C
55 °C
60 °C
Retention time (minutes)

Figure 1

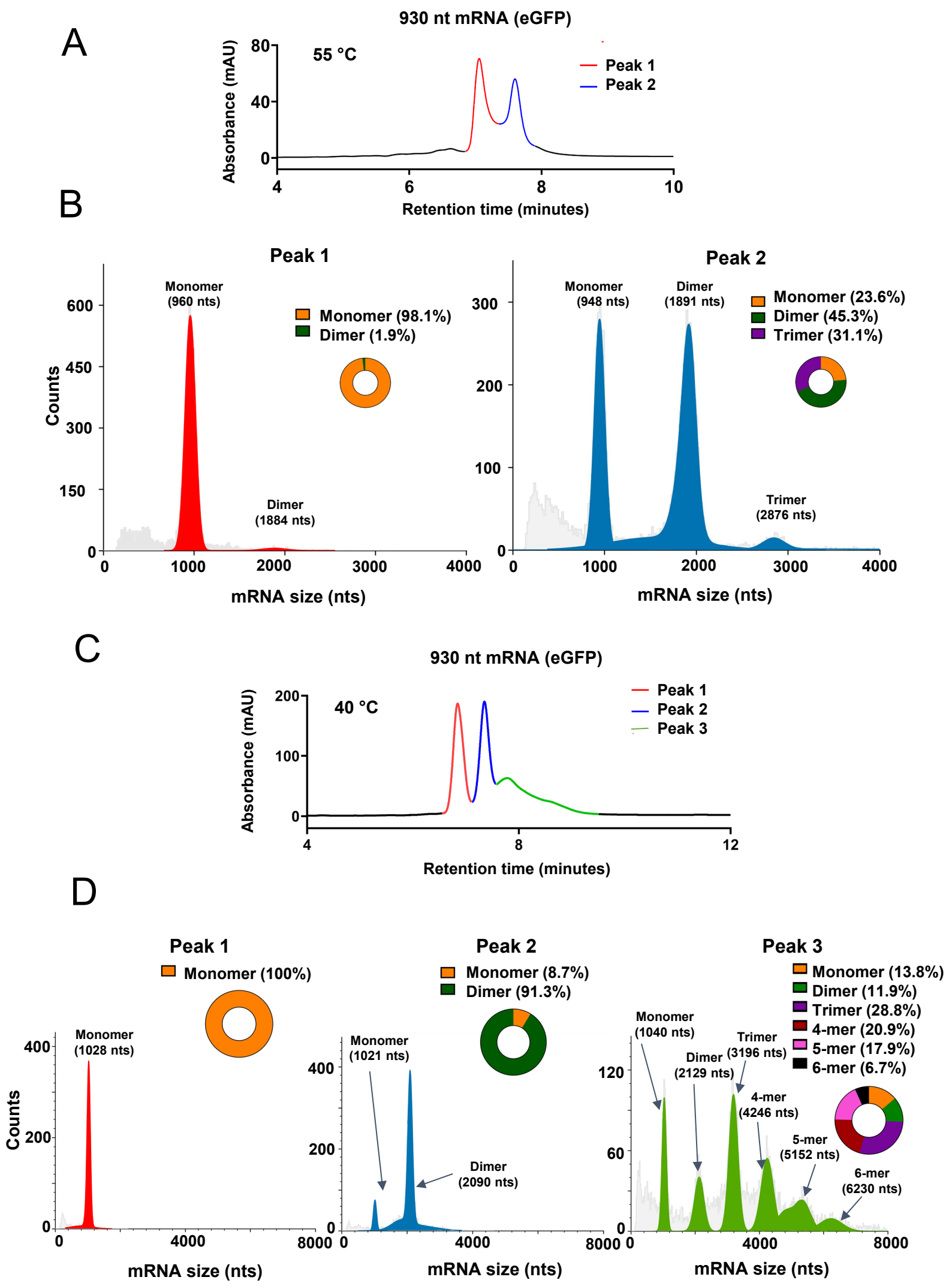
A
930 nt mRNA (eGFP)
55 °C
Peak 1
Peak 2
Absorbance (mAU)
Retention time (minutes)
B
Peak 1
Monomer (960 nts)
Monomer (98.1%)
Dimer (1.9%)
Dimer (1884 nts)
Counts
mRNA size (nts)
Peak 2
Monomer (948 nts)
Dimer (1891 nts)
Monomer (23.6%)
Dimer (45.3%)
Trimer (31.1%)
Trimer (2876 nts)
mRNA size (nts)
C
930 nt mRNA (eGFP)
40 °C
Peak 1
Peak 2
Peak 3
Absorbance (mAU)
Retention time (minutes)
D
Peak 1
Monomer (100%)
Monomer (1028 nts)
Counts
mRNA size (nts)
Peak 2
Monomer (8.7%)
Dimer (91.3%)
Monomer (1021 nts)
Dimer (2090 nts)
mRNA size (nts)
Peak 3
Monomer (13.8%)
Dimer (11.9%)
Trimer (28.8%)
4-mer (20.9%)
5-mer (17.9%)
6-mer (6.7%)
Monomer (1040 nts)
Dimer (2129 nts)
Trimer (3196 nts)
4-mer (4246 nts)
5-mer (5152 nts)
6-mer (6230 nts)
mRNA size (nts)

Figure 2

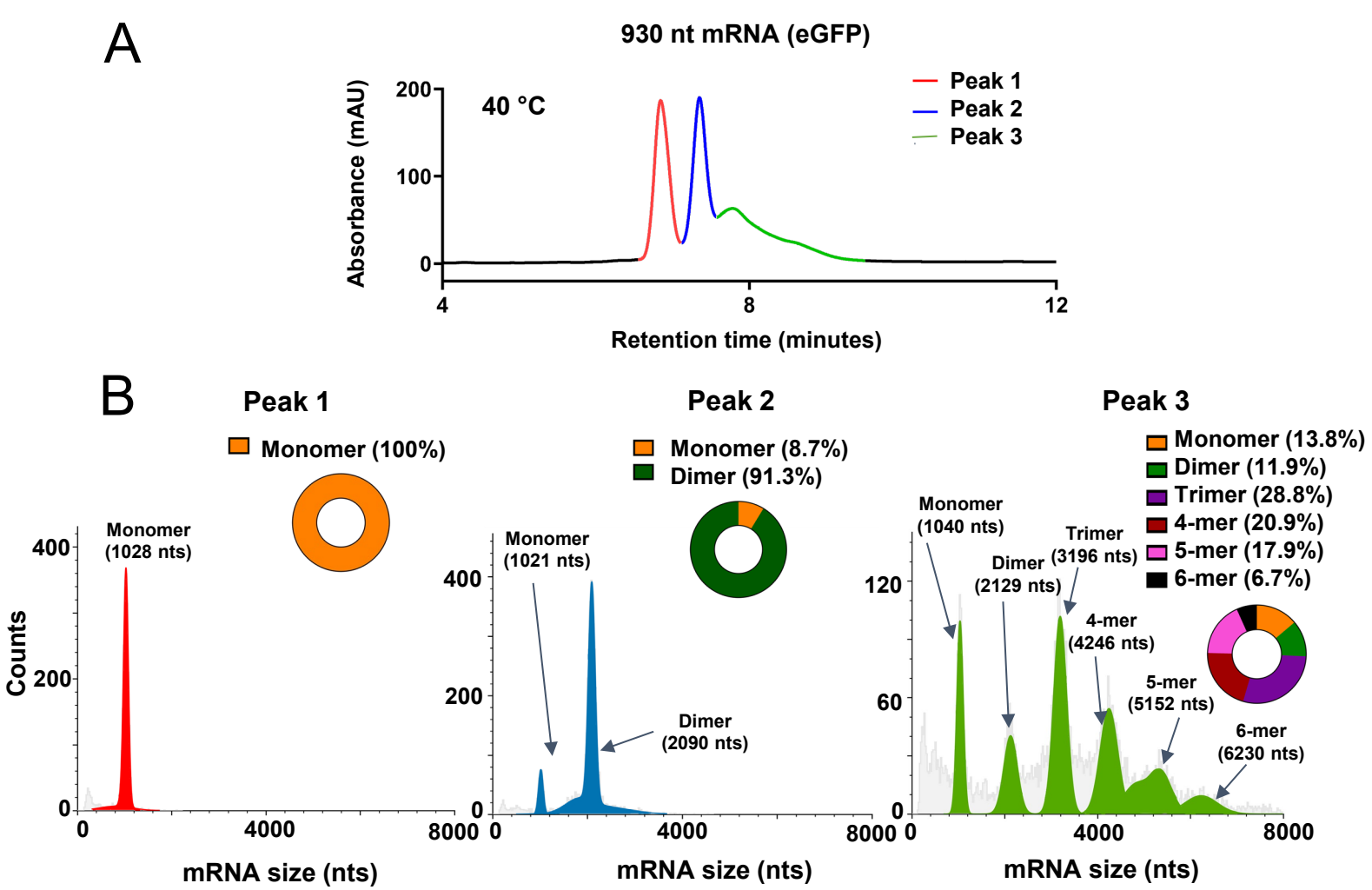
A
930 nt mRNA (eGFP)
40 °C
Peak 1
Peak 2
Peak 3
Absorbance (mAU)
200
100
0
4
8
12
Retention time (minutes)
B
Peak 1
Monomer (100%)
Monomer
(1028 nts)
Peak 2
Monomer (8.7%)
Dimer (91.3%)
Monomer
(1021 nts)
Dimer
(2090 nts)
Peak 3
Monomer (13.8%)
Dimer (11.9%)
Trimer (28.8%)
4-mer (20.9%)
5-mer (17.9%)
6-mer (6.7%)
Monomer
(1040 nts)
Dimer
(2129 nts)
Trimer
(3196 nts)
4-mer
(4246 nts)
5-mer
(5152 nts)
6-mer
(6230 nts)
Counts
400
200
0
120
60
0
4000
8000
mRNA size (nts)

Figure 2

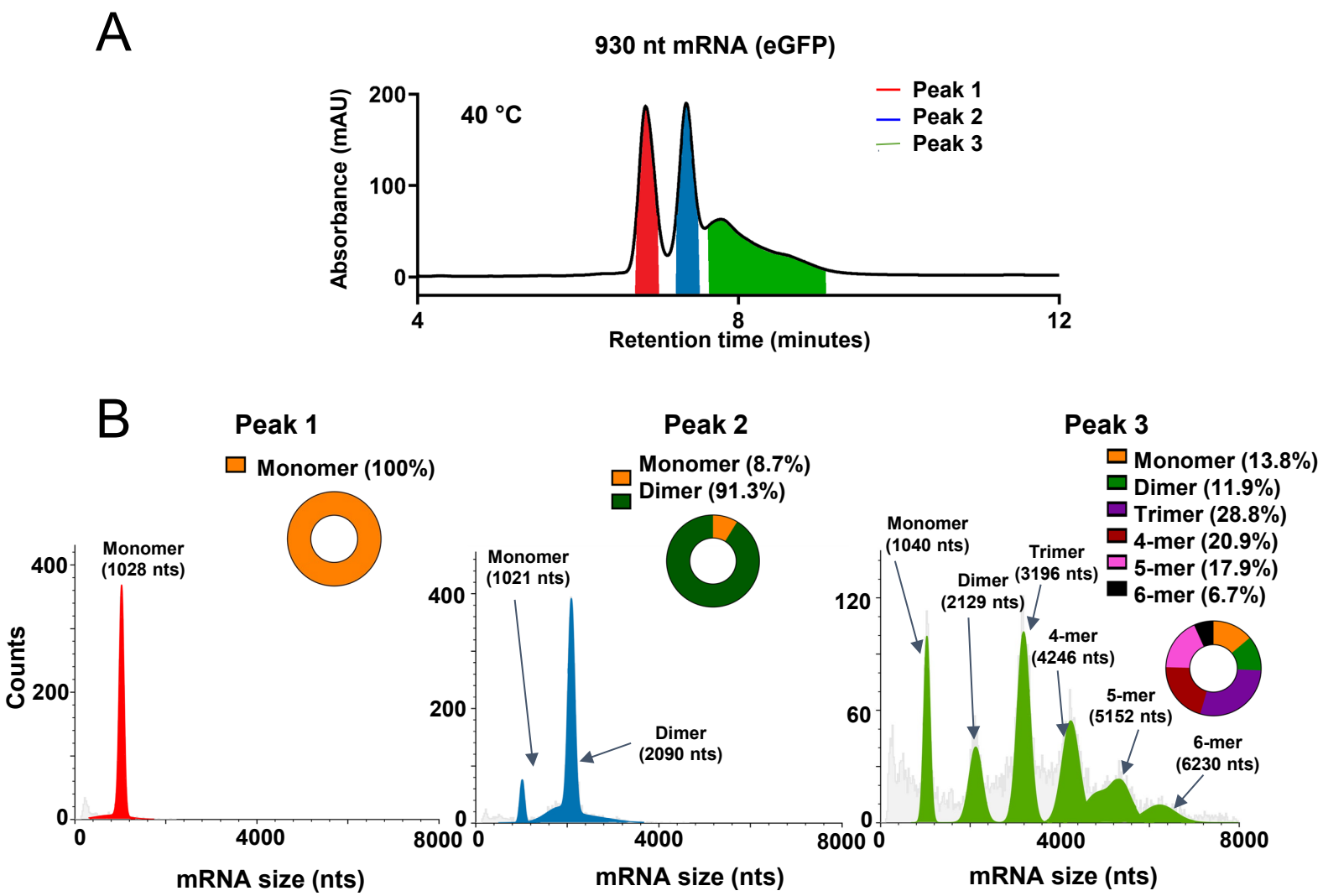
A
930 nt mRNA (eGFP)
40 °C
Peak 1
Peak 2
Peak 3
Absorbance (mAU)
200
100
0
4
8
12
Retention time (minutes)
B
Peak 1
Monomer (100%)
Monomer
(1028 nts)
Counts
400
200
0
0
4000
8000
mRNA size (nts)
Peak 2
Monomer (8.7%)
Dimer (91.3%)
Monomer
(1021 nts)
Dimer
(2090 nts)
400
200
0
0
4000
8000
mRNA size (nts)
Peak 3
Monomer (13.8%)
Dimer (11.9%)
Trimer (28.8%)
4-mer (20.9%)
5-mer (17.9%)
6-mer (6.7%)
Monomer
(1040 nts)
Dimer
(2129 nts)
Trimer
(3196 nts)
4-mer
(4246 nts)
5-mer
(5152 nts)
6-mer
(6230 nts)
120
60
0
0
4000
8000
mRNA size (nts)

Figure 2

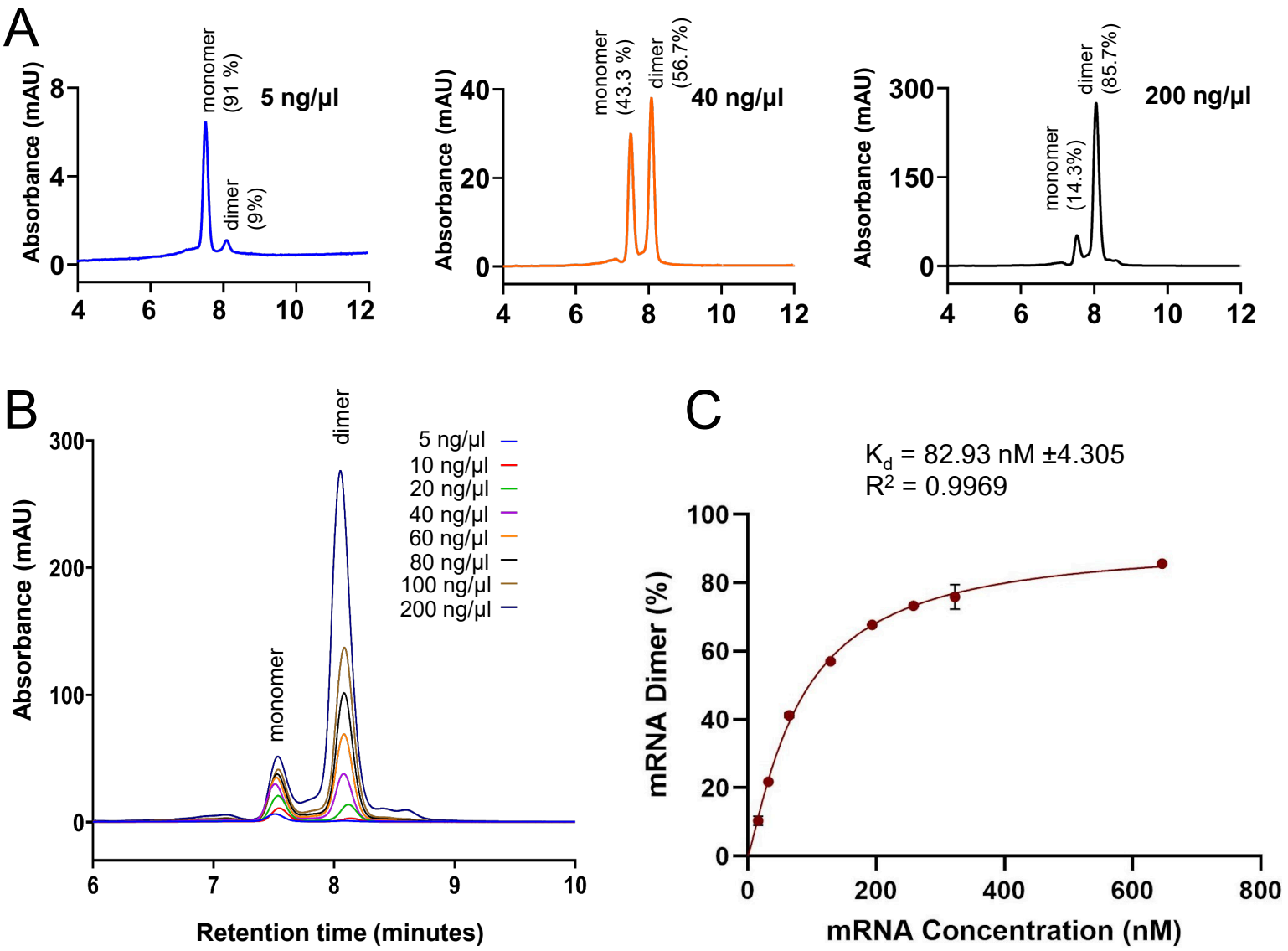
A
Absorbance (mAU)
monomer (91 %)
dimer (9%)
5 ng/µl
monomer (43.3 %)
dimer (56.7%)
40 ng/µl
monomer (14.3%)
dimer (85.7%)
200 ng/µl
B
Absorbance (mAU)
monomer
dimer
5 ng/µl
10 ng/µl
20 ng/µl
40 ng/µl
60 ng/µl
80 ng/µl
100 ng/µl
200 ng/µl
Retention time (minutes)
C
K_d = 82.93 nM ±4.305
R^2 = 0.9969
mRNA Dimer (%)
mRNA Concentration (nM)

Figure 3

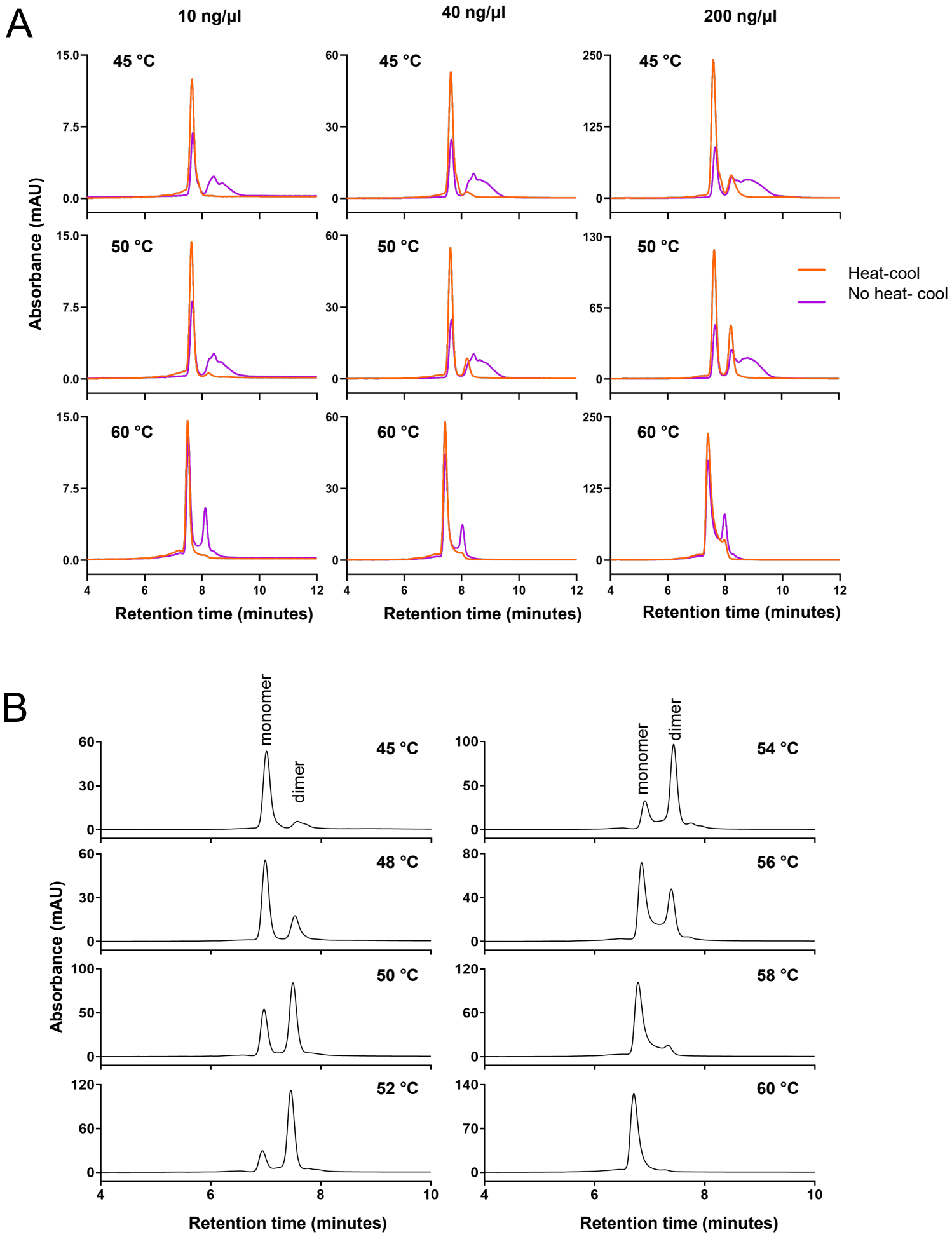
A
10 ng/µl
40 ng/µl
200 ng/µl
45 °C
50 °C
60 °C
Absorbance (mAU)
Retention time (minutes)
Heat-cool
No heat- cool
B
monomer
dimer
45 °C
48 °C
50 °C
52 °C
54 °C
56 °C
58 °C
60 °C
Absorbance (mAU)
Retention time (minutes)

Figure 4

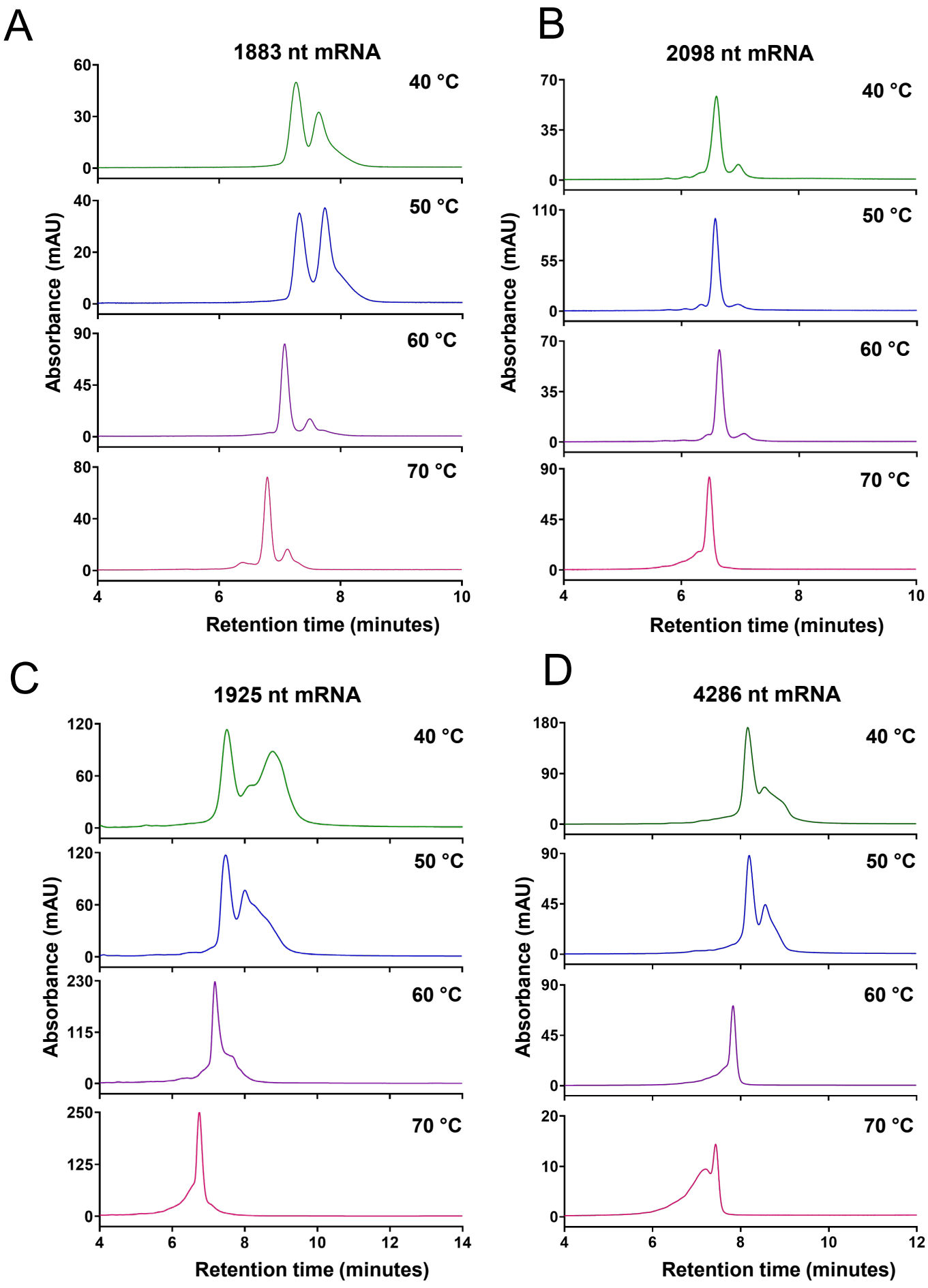
A
1883 nt mRNA
40 °C
50 °C
60 °C
70 °C
Absorbance (mAU)
Retention time (minutes)
B
2098 nt mRNA
40 °C
50 °C
60 °C
70 °C
Absorbance (mAU)
Retention time (minutes)
C
1925 nt mRNA
40 °C
50 °C
60 °C
70 °C
Absorbance (mAU)
Retention time (minutes)
D
4286 nt mRNA
40 °C
50 °C
60 °C
70 °C
Absorbance (mAU)
Retention time (minutes)

Figure 5

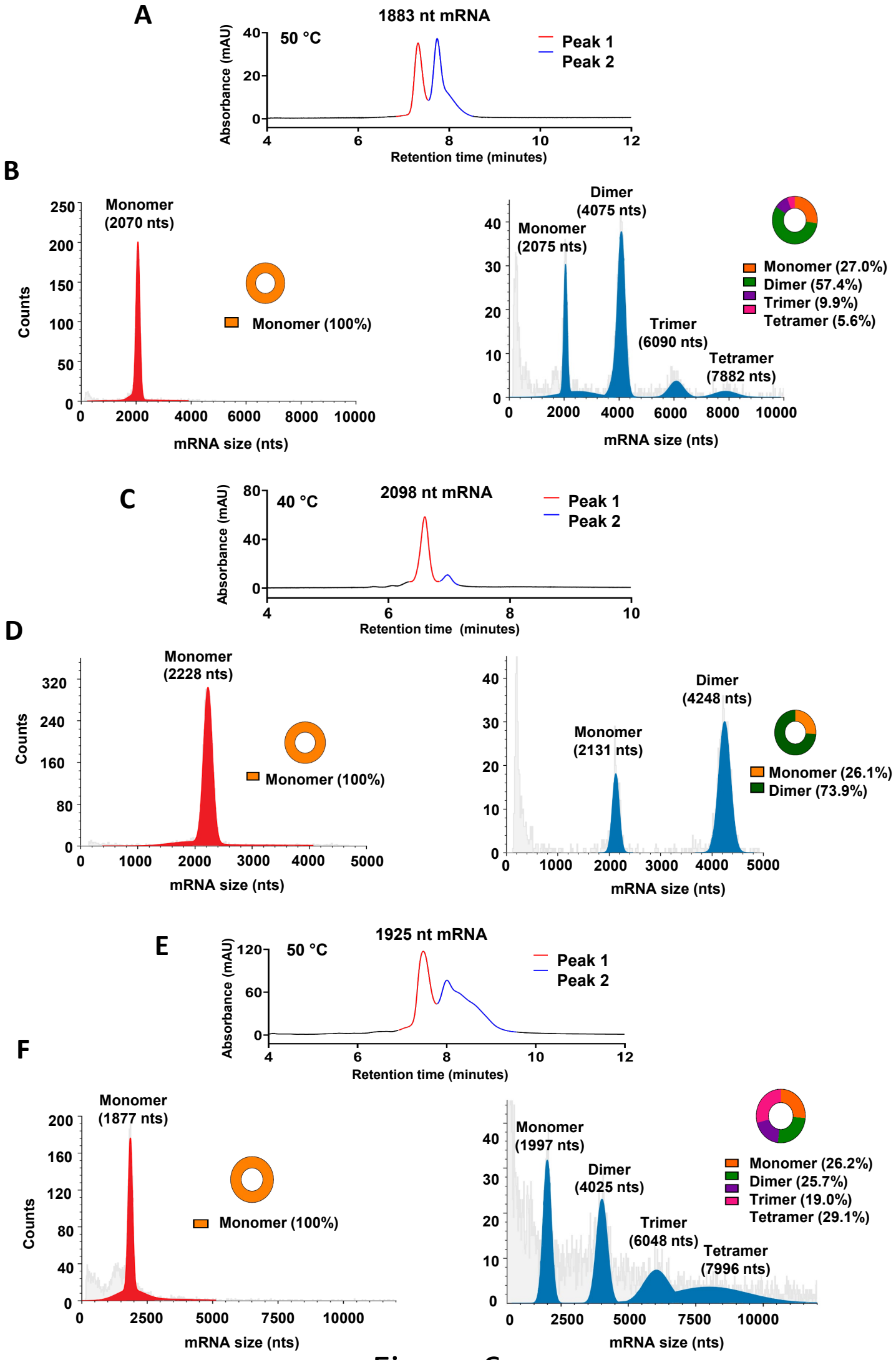
A
1883 nt mRNA
50 °C
Peak 1
Peak 2
Absorbance (mAU)
Retention time (minutes)
B
Monomer
(2070 nts)
Monomer (100%)
Counts
mRNA size (nts)
Dimer
(4075 nts)
Monomer
(2075 nts)
Trimer
(6090 nts)
Tetramer
(7882 nts)
Monomer (27.0%)
Dimer (57.4%)
Trimer (9.9%)
Tetramer (5.6%)
C
2098 nt mRNA
40 °C
Peak 1
Peak 2
Absorbance (mAU)
Retention time (minutes)
D
Monomer
(2228 nts)
Monomer (100%)
Counts
mRNA size (nts)
Dimer
(4248 nts)
Monomer
(2131 nts)
Monomer (26.1%)
Dimer (73.9%)
E
1925 nt mRNA
50 °C
Peak 1
Peak 2
Absorbance (mAU)
Retention time (minutes)
F
Monomer
(1877 nts)
Monomer (100%)
Counts
mRNA size (nts)
Monomer
(1997 nts)
Dimer
(4025 nts)
Trimer
(6048 nts)
Tetramer
(7996 nts)
Monomer (26.2%)
Dimer (25.7%)
Trimer (19.0%)
Tetramer (29.1%)

Figure 6